Composites Part A 130 (2020) 105765

Contents lists available at ScienceDirect

Composites Part A

journal homepage: www.elsevier.com/locate/compositesa

Interfacial crystals morphology modification in cellulose fiber/polypropylene composite by mechanochemical method

Lang Huang[a,b,c], Qiong Wu[b,*], Qingwen Wang[d], Michael Wolcott[c,*]

[a] Qingdao Industrial Energy Storage Research Institute, Qingdao Institute of Bioenergy and Bioprocess Technology, Chinese Academy of Sciences, Qingdao 266101, China
[b] Cultivation Base of State Key Laboratory of Ecological Chemical Industry, College of Chemical Engineering, Qingdao University of Science and Technology, 53 Zhengzhou Road, Qingdao, Shandong Province 266042, China
[c] Composite Material and Engineering Center, Washington State University, 2001 East Grimes Way, Pullman, WA 99164, USA
[d] College of Materials and Energy, South China Agricultural University, 483 Wushan Road, Guangzhou 510642, China

ARTICLE INFO

Keywords:
Polymer-matrix composites (PMCs)
Interface/interphase
Micro-mechanics
Mechanical testing

ABSTRACT

The insufficient interfacial bonding and low toughness of cellulosic fiber reinforced polypropylene (PP) composite remain limitations for advanced applications of the composite. Here we proposed to promote the interfacial adhesion by modifying the interfacial matrix crystal type and morphology, inducing the small β -PP spherulite from the dominated α-PP. Specifically, cellulose fiber was subjected to mechanical milling to improve the accessibility of hydroxyl groups, then pimelic acid, calcium carbonate and activated cellulose particles were mechanochemically reacted during solvent-free ball milling condition to prepare cellulose fillers with β nucleating sites for PP reinforcement. The nucleating effect and tensile properties of the composite were investigated. The results showed that the modified particles were effective for producing a large percentage of β crystals with smaller and more uniform spherulite, and the induced β phase crystal increased the tensile strength and elongation at break of the composite.

1. Introduction

Cellulosic fiber from agricultural and forest sources has been widely utilized to replace synthetic or mineral filler for reinforced polymer composites due to their availability, renewable nature, low cost, and light weight [1,2]. The performance of fiber reinforced composites is usually determined by the properties of the reinforcing agent, the matrix, and their interfacial adhesion quality. Basically, the surface appearance, environmental tolerance and durability of natural fiber reinforced polymer composites depend mainly on the matrix, while the fibrous reinforcements provide macroscopic stiffness and strength. Polypropylene (PP) is widely used as a matrix for composites due to its well-balanced mechanical property and ease of processing. However, when incorporated with low L/D ratio particles, the natural fiber reinforced PP composites generally suffer toughness decrease, which limited their utilization in demanding applications. Adding coupling agents could increase the strength and stiffness of the composite, but on the other hand, often lead to decrease of the impact properties [3–5]. The matrix microstructure, the crystal morphology that includes spherulites size, and interface crystallization, has a significant influence on determining the toughness performance of the composites [6,7].

As a semi-crystalline plastic, isotactic PP has three different morphological crystal forms, α, β, and γ, which can be obtained from different preparation procedures [8,9]. Among them, α-PP is by far the most common form and occurs under a wide variety of crystallization conditions, β-PP is thermodynamically metastable, and γ-PP is rare and difficult to obtained [10]. β-PP has received much attention for its unique crystal structure that leads to high impact resistance [11,12]. Previous researches have demonstrated that β-nucleated PP composites showed increased notched impact strength and heat distortion temperatures [13–17]. Numerous methods have been applied to produce large quantities of the β phase. To date, adding β-nucleating agents has proven to be the easiest and most effective method to prepare high fractions of β-PP [18]. Several organic or inorganic β nucleating agents, including pigments [19], aromatic amide compounds [2,20], or some certain metal salts and their mixture with specific dicarboxylic acids [13,14], are reported with high β-PP nucleating efficiency. Pimelate salts became attractive for its high thermal stability and excellent PP β-crystal nucleating ability recently. Meng et al. [21] studied pimelic acid as a surface modifier for wollastonite and the results showed that treated wollastonite induced the formation of β-phases PP. Gonzalez-Calderon et al. [22] and Wang et al. [23] used pimelate salts to

* Corresponding authors.
E-mail addresses: wuqiong0506@hotmail.com (Q. Wu), wolcott@wsu.edu (M. Wolcott).

https://doi.org/10.1016/j.compositesa.2020.105765
Received 11 August 2019; Received in revised form 7 November 2019; Accepted 5 January 2020
Available online 07 January 2020
1359-835X/

functionalize multi-walled carbon nanotubes with the nucleating agent and found increased β crystal content in PP matrix.

Most available research regarding natural fiber filled PP composites has focused on improving the interfacial incompatibility by fiber surface modifications or adding coupling agents [24–29]. However, few of these studies have addressed the matrix crystal type or morphology. For the cellulose fiber, each D-anhydroglucopyranose unit possesses three hydroxy groups at C2, C3, and C6 position, which are potentially capable for a variety of chemical modifications [30]. However, due to highly organized crystal structure and the huge molecular mass, the reaction availability of the hydroxyl groups is extremely low during chemical modifications [31]. Traditional way to activate cellulose is breaking or weakening the interconnected hydrogen bonds with swelling agents such as N,N-dimethyl formamide and dimethyl sulfoxide, but use of such agents appear to be increasingly unsustainable because they are hazardous, non-eco-friendly, and energy-demanding for the solvent production, purification and recycling [32–34].

Here mechanical ball milling was employed as a solvent-free approach to disintegrate the interconnections, reduce the crystallinity, promote the availability of the hydroxyl group from cellulose fiber [35]. In addition, selected chemicals, pimelic acid (heptanedioic acid) and calcium carbonate, were added during ball milling to react with cellulose for later inducing the β-phase in PP composites. Acetic anhydride was used to form mixed anhydrides with pimelic acid for improved reactivity. The nucleator synthesis was then characterized. Finally, the modified powder filled PP composites were prepared, and the crystallization behavior, crystal structure, mechanical property and spherulite morphology were investigated.

2. Experimental

2.1. Materials

Cellulose particle was prepared from northern softwood bleached kraft pulp (Sigma Aldrich, MO, USA). Pimelic Acid, 98%, $HO_2C(CH_2)_5CO_2H$, and light powder calcium carbonate, 98% pure, with an average particle diameter of 20 μm, were purchased from Fisher Scientific, MA, USA. Acetic anhydride (≥99%, Sigma Aldrich, MO, USA) was used as co-reagent and sodium hypophosphite (NaH_2PO_2, Sigma Aldrich, MO, USA) was employed as the catalyst for the reaction. Polypropylene, (Melt Flow, 4 g/10 min, Fortilene HB9200, BPSolvay Polymers, TX, USA), was used as the matrix for the composite preparation.

2.2. Cellulose pulverization and activation

A planetary ball mill (Across international, PQ-N04) with two 100-mL stainless steel jars and stainless balls was used to pulverize and activate cellulose fibers. Different ball milling time of 10, 30 and 60 min were empolyed to investigate the morphology and crystal structure change of cellulose.

2.3. Sample modification

As illustrated in Fig. 1, cellulose fibers were ball milled for 30 min to prepare active powder. Acetic anhydride (AA), pimelic acid (PA) and calcium carbonate were added into the milling jar and co-milled with the cellulose powder (CP) for 120 min at ambient temperature and pressure. The molar ratio of the components used in the reaction was AA: PA: $CaCO_3$: CP = 2:2:1:2. Sodium hypophosphite (10%) was added with cellulose powder as the catalyst. All the solid particles were dried at 80 °C before use. After milling, the residual was washed with ethanol and DI water, then Soxhlet extracted for 5 days to completely remove the unreacted chemicals. The filtered modified cellulose powder (MCP) was dried at 80 °C overnight and then characterized.

2.4. Composites preparation

Modified cellulose powders were oven dried at 80 °C (Across International Oven, NJ, USA) until reaching a constant weight and subsequently dry blended with PP at a cellulose weight ratio of 5%, 10% and 20%. The dry blend was then compounded using a Haake mini lab (Thermo Scientific, Dreieich, Germany) at a mixing temperature of 175 °C, with a rotational speed of 90 rpm, for 15 min. After air cooling, the extruded strands were pelletized and collected for injection molding. Standard tension specimens ($3.18 \times 9.53 \times 1.5$ mm^3 for the narrow section) were injection molded using a Haake mini-Jet (Thermo Scientific, Dreieich, Germany), with a cylinder temperature of 190 °C and a pressure of 650 bar. After the injection, samples were kept in the 70 °C mold for 25 s at a hold pressure of 250 bar. All the samples were stored at room temperature and humidity for one week before testing. Samples of neat PP, 10% unmodified cellulose particle composites (CP/PP), and 10% calcium carbonate filling composite ($CaCO_3$/PP) were prepared using the same process condition.

2.5. Characterizations

2.5.1. Cellulose particle size, morphology and crystallinity

A laser scattering particle size analyzer (Malvern instrument, Worcestershire, UK) was used to evaluated the paricle size and distribution of the ball milled cellulose fiber. The d_{50}, 50% percentiles from the cumulative size distribution, is used to act as the average particle diameter size, while the Δd ($\Delta d = d_{90} - d_{10}$) is used to represent the dimensionless value to analyze the broadness of the particle size distribution.

The morphology of the milled particle was analyzed by scanning electron microscopy (SEM). Cellulose particles were dried and surface-coated with gold before imaging. Pictures were taken at 20 kV accelerating voltage (FEI Quanta 200F, field emission gun ETD detectors, FEI Company, Oregon, USA).

The cellulose crystal structure and crystallinity was investigated with an X-ray diffractometer (XRD, Rigaku, mini flex 600, Tokyo, Japan), equipped with a Cu kα (λ = 0.154 nm), radiated from 40 kV and 15 mA. The testing 2θ ranges from 10 to 40° and the relative degree of crystalline, (*CrI*), was calculated employing the Eq. (1) [36].

$$CrI\% = [(I_{002} - I_{am})/I_{002}] \times 100 \quad (1)$$

where I_{002} is the intensity of the peak located around 22.6° and I_{am} refers to the minimum intensity between the main (22.6°) and secondary peaks (16.1°).

2.5.2. Modification characterizations

A Fourier transform infrared (FT-IR) spectrometer (Nicolet Nexus 670 spectrometer, Thermo Fisher Scientific, USA) was employed to conduct the FT-IR test. Sample discs were produced using a laboratory pellet press and the pellet mold, mixed with KBr at a mass ratio of cellulose powder: KBr = 1:100. Spectra were collected at a resolution of 4 cm^{-1} and 64 scans, ranged from 500 to 4000 cm^{-1}. The solid-state CP/MAS ^{13}C Nuclear magnetic resonance (NMR) analysis was conducted on an Agilent DD2 600 MHz NMR spectrometer (Agilent CA, USA). Samples were tested at a spinning rate of 6 kHz, with solid powder filled into the tested probe.

Thermogravimetric analysis (TGA) was carried out via a SDT-Q600 instrument (TA instrument, DE, USA). An alumina crucible was used to hold the 10 mg sample and the temperature was ramped from 25 to 600 °C with a 10 °C/min rate under a nitrogen atmosphere, with a flow rate of 100 μL/min.

2.5.3. Composite characterizations

The melting and crystallization properties were investigated using the differential scanning calorimeter (DSC, Perkin Elmer, MA, USA). Approximately 8 mg samples of PP and PP composites were capsuled

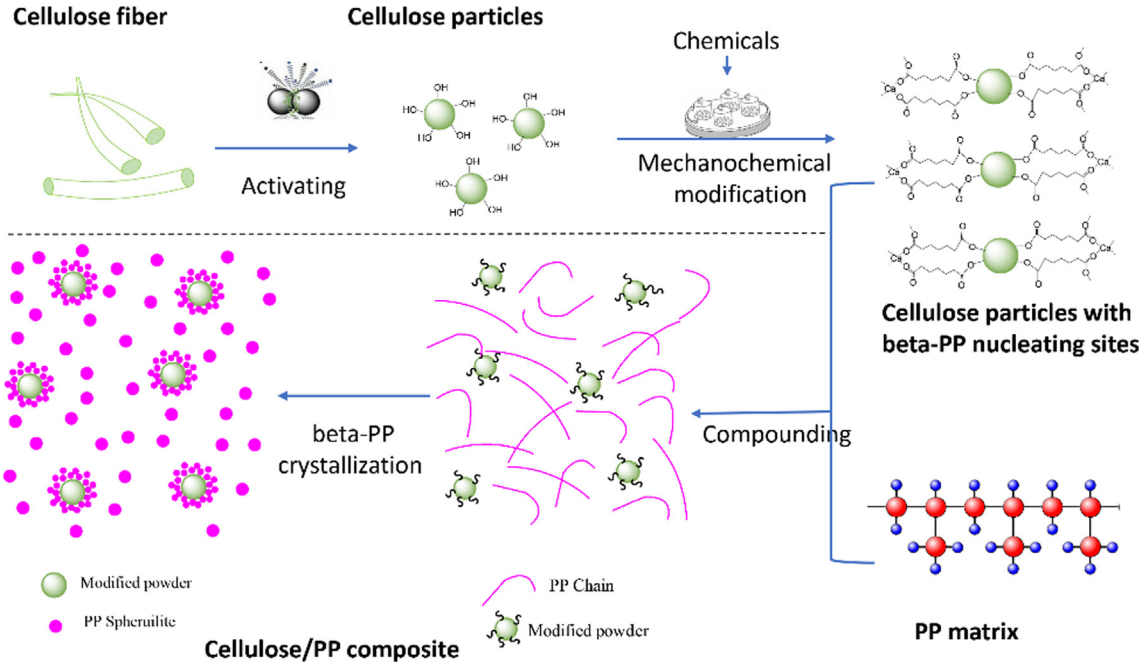

Fig. 1. Schematic diagrams of the mechanochemical way to prepare spherulite-controlled PP composites. (For interpretation of the references to color in this figure legend, the reader is referred to the web version of this article.)

into aluminum crucibles (40 μL, Mettler Toledo, OH, USA). The temperature was heated rapidly (20 °C/min) to 210 °C, held for 5 min to erase previously thermal history, then cooled to 50 °C and reheated to 200 °C at 10 °C/min. All procedures were conducted under an N_2 atmosphere.

An X-ray diffractometer (Rigaku, mini flex 600, Tokyo, Japan) with a Cu kα (λ = 0.154 nm) radiation source generated at 40 kV and 15 mA, was employed to analyze the crystal structure of the reinforced composites. The instrument scanning 2θ range was from 5 to 25°.

The crystallization morphology was investigated by an Olympus BX51 polarized optical microscopy, attached with a DP70 digital camera (Olympus, Tokyo, Japan) and a THMS600 hot stage (Linkam, UK). A thin slice, cryo-microtomed from the composite with a glass knife, was placed between two glass slides, then heated on the hot stage. The temperature was rapidly raised to 210 °C at 20 °C/min and held for 5 min, then cooled at 5 °C/min to 25 °C, and the spherulite morphology was observed.

The tensile performance of the composites was tested using the injection molded standard tension specimens in a universal testing machine with a 10 kN electronic load cell and an MTS 634.12 × 10^{-24} extensometer (Instron 4466, Canton, OH, USA). All testing was conducted in accordance with ASTM D638 [37] with five replicates samples for each formulation.

3. Results and discussion

3.1. Cellulose activation from ball milling

Controlling the crystallinity of cellulose is the prerequisite for cellulose chemical modification. Here, the effect of the mechanical planetary ball milling on breaking down the intra/inter connection was studied. As shown in Fig. 2(a), 10 min of ball milling successfully broke down the long cellulose fiber into short ones, with an average particle size (d_{50}) of 162 μm and a Δd value of 516. After 30 min ball milling, the particles keep reducing and the average particle size value is 71 μm and the Δd is 121, while d_{50} = 42 μm and Δd = 88 for cellulose particles after 60 min ball milling. In addition, the morphology of particle also changed during the ball milling, long fibers were broken into short fiber in the early milling stage, and then turned into ellipsoid particles with an aspect ratio of *ac.*1 after further milling. In the planetary ball milling process, longer milling time correlated to the higher energy input allows for more collisions between the milling balls, filler materials and the chamber wall, leading to smaller and more uniform particles.

The crystal structure of the cellulose particle during ball milling were also investigated. As depicted in Fig. 2(d), before milling, two characteristic signal peaks centered at 2θ = 16.1° and 22.6° appeared, which refer to the (1 0 1) and (0 0 2) diffraction planes of cellulose crystalline structure [38]. After 10 min ball milling, the intensities of these two peaks weakened, demonstrating the undergoing of the de-crystallization of cellulose fiber concurrent with size reduction. After 30 and 60 min of ball milling, the main peak shifting implies that the crystalline region of cellulose was destroyed and amorphous cellulose particles were resulted. For cellulose, the inter/intra hydrogen bonds are mainly response for the three-dimensional crystal structures. During the ball milling, mechanical collisions broken down long fibers into micro-particles, destroying the interconnected hydrogen bonds and leading to the amorphous cellulose. The improved specific surface area from fiber pulverization as well as the de-crystallinity of cellulose during ball milling would be beneficial for the later cellulose surface chemical modifications.

3.2. Mechanochemistry reaction characterization

A proposed reaction scheme for the grafting of cellulose particles is illustrated in Fig. 3. FTIR was used to assess the resulting bonds and the spectra were presented in Fig. 4(a). For unmodified cellulose particles, the broad absorption peak at 3100–3600 cm^{-1} is attributed to the O-H stretching vibration and the hydrogen bond from the hydroxyl groups. The peak located at *ca.* 2900 cm^{-1} is related to the C—H stretching vibration from CH and CH_2, and the peaks at *ca.* 1644, 1380 and 1100 cm^{-1} are related to the fiber-OH from the absorbed water, the aryl-alkyl ether and pyranose ring skeletal C—O—C and the C—OH groups, respectively [39]. The spectra of pimelic acid was also provided as a control. For pimelic acid, the bands at 1709 and 1275 cm^{-1} were attributed to the C═O and C—O stretching vibrations. After the

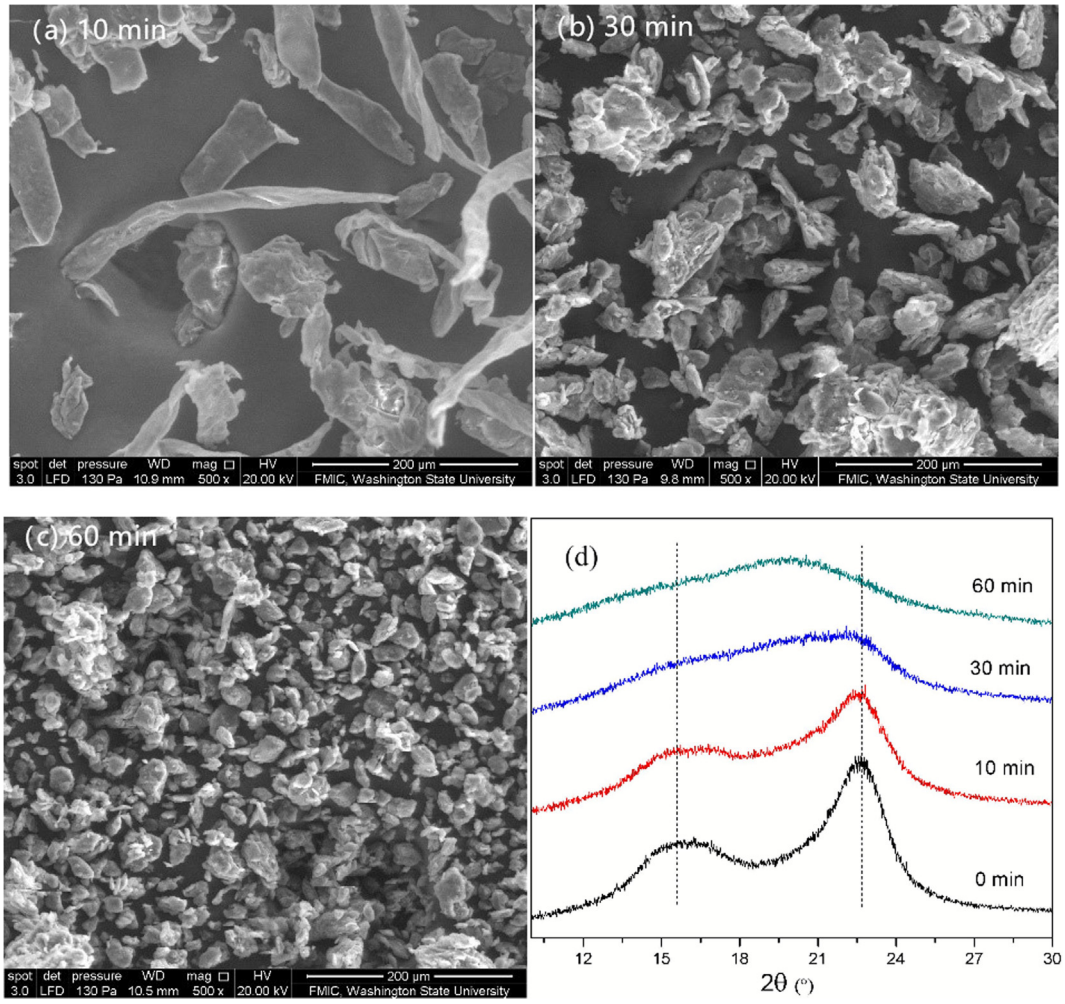

Fig. 2. SEM images of milled particles (a, b, c: 10, 30, 60 min ball milled) and their XRD curves (d). (For interpretation of the references to color in this figure legend, the reader is referred to the web version of this article.)

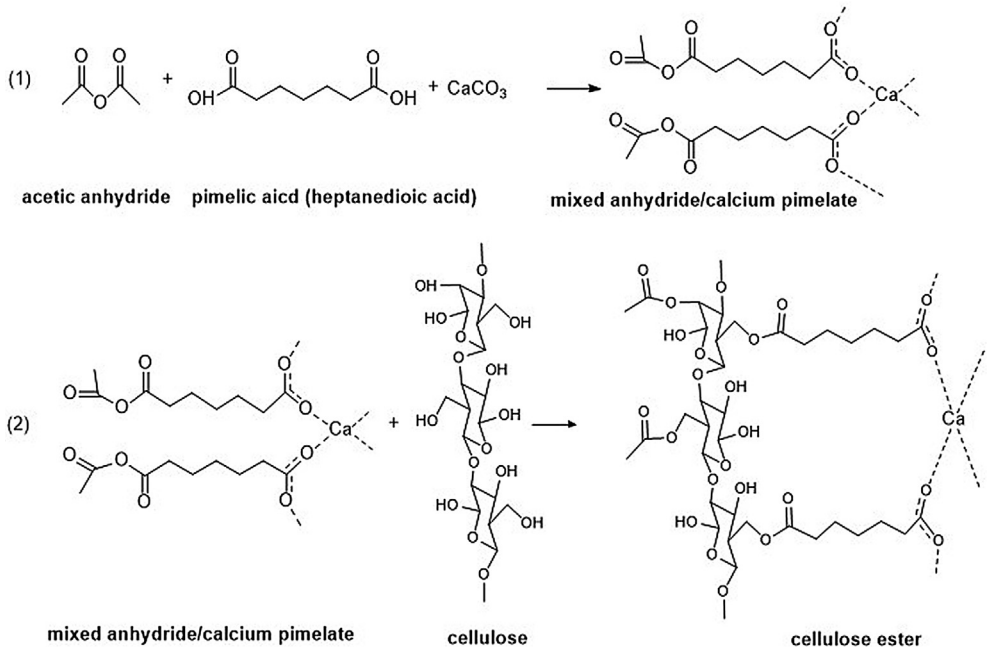

Fig. 3. Proposed mechanism for the functionalization of active cellulose powder.

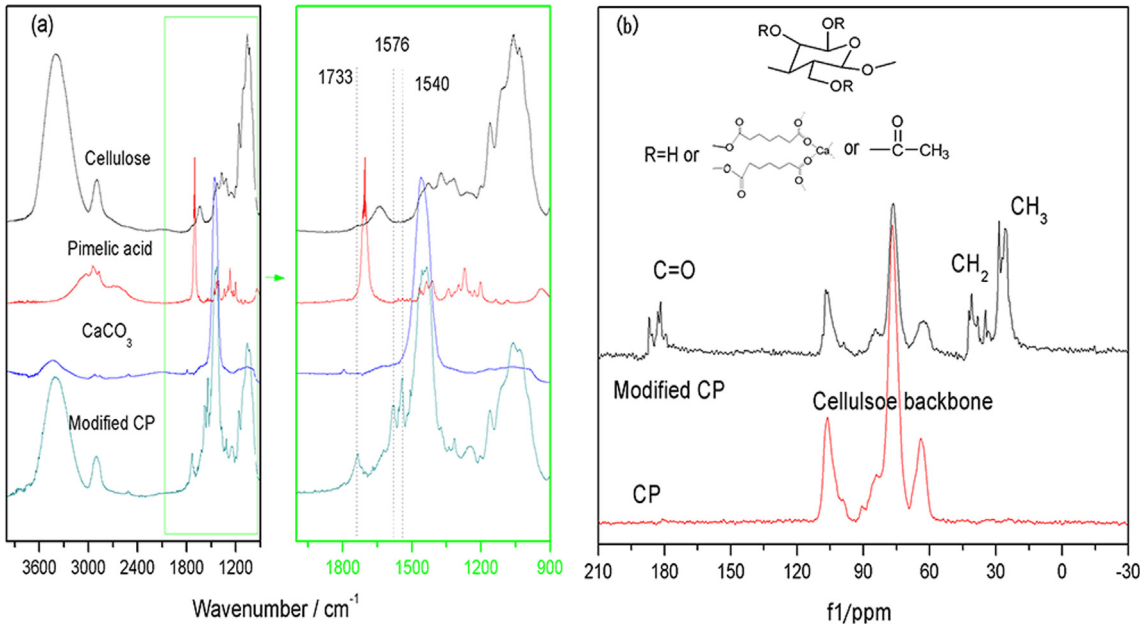

Fig. 4. FT-IT (a) and solid-state CP/MAS ^{13}C NMR spectra (b) of the modified cellulose powder. (For interpretation of the references to color in this figure legend, the reader is referred to the web version of this article.)

mechanochemical modification, three new peaks appeared on the modified cellulose. The peak located at 1733 cm^{-1} is attributed to the C═O stretching from the ester bond, indicating the occurrence of the cellulose esterification. In addition, two peaks at 1576 and 1540 cm^{-1} could be observed and are assigned to the dissymmetry stretching vibration of COO− from calcium pimelate [13]. Therefore, during the mechanochemical ball milling reaction, the −COOH was reacted with the calcium ion and formed the calcium salts.

To further investigate the structure of the modified cellulose powders, solid-state ^{13}C NMR was employed to provide detail information of the reaction. Spectra of cellulose powder and modified samples were presented in Fig. 4(b) and peak assignments were illustrated according to literatures [40–42]. For native cellulose, noticeable signals observed at 60–110 ppm were attributed to the carbon atoms of the glucopyranose rings from the cellulose backbone. After modifications, all the characteristic peaks at 60–110 ppm from the cellulose backbone were shown, with lower peak intensity than that of pure cellulose powder, indicating the cellulose main structure remained after the modification. However, several new peaks emerged for the MCP spectra. Peaks located at 180–190 ppm were corresponding to the carbon atoms from carbonyl (−C═O), while the peaks located at 10–30 ppm were attributed to the carbon atoms from the CH_2 and CH_3 groups. The NMR results demonstrated the formation of calcium pimelate and esterification of the cellulose were successfully achieved during the mechanochemical process, in agreement with the FTIR analysis.

3.3. Thermal degradation

The thermal degradation behavior of the modified samples was analyzed by TGA & DTG. The result was shown in the following Fig. 5, and the mass loss in different degradation stages was summarized in Table 1. It can be observed that the pimelic acid degraded completely between 155 and 295 °C. In contrast, the calcium carbonate is an inorganic material and exhibited a high initial degradation temperature of 630 °C. Between 630 and 770 °C, the $CaCO_3$ were degraded into CaO and exhibited a mass loss of 41.4%. The pure cellulose particles displayed an initial decomposition temperature of 240 °C and the main decomposed temperature ranged from 240 to 375 °C, along with a 79.4% mass loss. The modified samples presented three degradation stages. The first mass loss occurred at 210–367 °C, corresponding to the decomposition of cellulose backbone structure. The lower initial degradation temperature was attributed to the influence of the grafted pimelic acid chains, as reported by other researchers [35,43]. The increase of the grafted carbon chain length of cellulose esters followed with the decrease of the thermal stability, also implies the occurrence of the esterification during ball milling [44]. Meanwhile, a complete new degradation stage (stage II) at 400–495 °C appeared, which was due to evaporating the organic substances along with the decomposition of calcium salts into $CaCO_3$. Finally, the degradation stage III from 630 to 720 °C was the evaporation of CO_2 produced by the decarboxylation process of $CaCO_3$.

3.4. Crystallization and melting behavior

Different types of PP crystals display different crystallization characteristics. In order to identify the nucleating effect of the modified particles on the crystallization behavior of the PP matrix, the crystallization and melting process were investigated by DSC (Fig. 6). For the cooling process (Fig. 6a), neat PP displayed a crystallization temperature (T_p) of 112.3 °C. After incorporating with 10% untreated particles, the T_p of the PP/CP and PP/$CaCO_3$ samples increased to 115.1 °C and 121.0 °C, respectively. These changes demonstrated that the filling particles could promote PP crystallization by the heterogeneous nucleating effect. The calcium carbonate particles, with a smaller size and narrower size distribution, exhibited more nucleating sites than that of cellulose particles, thereby providing a higher T_p. A 10% addition of MCP into the PP, further increased the T_p to 124.7 °C, indicating the stronger nucleating ability than those of CP and calcium carbonate filled composites. The modification changed the surface property of the particles, and the grafted nucleating sites with precise crystal nucleating sites providing sufficient time for the crystal growth, leading to an enhanced heterogenous nucleating effect. However, altering the filler content of the modified particles produced little change in the T_p, with 124.3 °C, 124.7 °C and 125.0 °C for 5%, 10% and 20% filler levels, respectively. This implies that after 5% filling percentage, further increase of filler concentration has limited influence on promoting the crystallization temperature.

The melting curves of PP and its filled composites are illustrated in Fig. 6b. A single main melting peak is located at *ca.* 165 °C for the neat PP and is attributed to the stable α phase PP crystal. The addition of

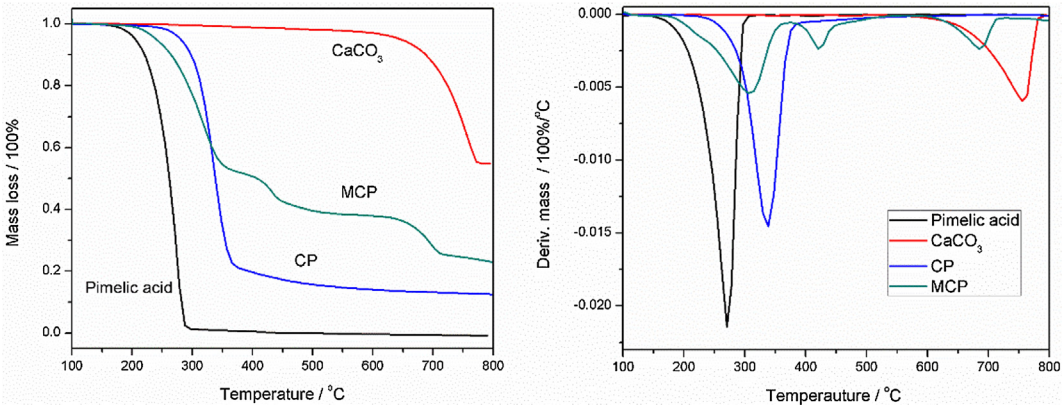

Fig. 5. TGA&DTG spectra of the modified cellulose powder. (For interpretation of the references to color in this figure legend, the reader is referred to the web version of this article.)

Table 1
Thermal degradation stages of the tested samples.

Samples	Degradation stages	Temperature range/°C	Mass loss/%
Pimelic acid	I	155–295	99.1
Calcium carbonate	I	630–770	41.4
Cellulose	I	240–375	79.4
Modified cellulose	I	210–367	46.3
	II	400–495	11.9
	III	630–720	11.3

untreated cellulose particles did not influence the melting behavior of the composites, indicating that CP did not affect the main crystal structure of the composite matrix. The $CaCO_3$/PP composite exhibited the same main peak at 165 °C, with a very small shoulder at 148 °C attributed to β form crystals, implying that adding the $CaCO_3$ particles also had little influence on matrix crystal type, producing predominately α PP crystals. However, when 10% modified CP filled the composite, two main peaks, one located at 165 °C and the other centered at 150 °C were revealed, representing the characteristic melting activities of the PP α and β form crystals, respectively [13,14,45]. The emergence of the peak at 150 °C indicated that the β PP was successfully induced by the modified particles in the composite. The percentages of the β crystal, K_β, determined by the peak area, were listed in Table 2. 57.33% β crystal was obtained by adding 10% modified CP, indicating the MCP was effective on transforming the PP crystal type from α to β. 5%, 10% and 20% MCP filled composites produced β crystal with the K_β values of 56.28%, 57.33% and 57.60%, respectively. This result implies that low MCP concentration has a sufficient β PP nucleating ability and increasing the MCP loading contents did not influence the β phase percentage in the composite. Generally, for particulate nucleating agents, there are two critical principles that need to be fulfilled to achieve highly efficient nucleating behavior: one is the lattice matching of the nucleators, the other is sufficient dispersion of the particles [46]. The high filler loading may increase particle agglomeration thereby reducing the effective nucleating density of the particles.

3.5. X-ray diffraction

X-ray diffraction diagrams also can provide information about the crystal structure. Here the XRD curves for PP and the composites were shown in Fig. 7. Pure PP displayed characteristic peaks at diffraction angles of 14°, 16.8°, 18.4°, 21.1°, 21.7°, attributed to the primary reflections of the (1 1 0), (1 4 0), (1 3 0), (1 3 1) and (1 1 1) planes of the α-PP crystal, respectively. The addition of the unmodified CP and $CaCO_3$ particles did not affect the peak locations, and the composites displayed similar spectra as that of pure PP, indicating that the effect of adding these fillers on the matrix crystalline structure was negligible. However, when the modified cellulose particles were incorporated with PP, pronounced peaks located at 15.9° and 20.9° appeared, corresponding to the reflection of the β crystal (3 0 0) and (3 0 1) planes, respectively, demonstrating the formation of the β crystal. Characteristic peaks of the β crystal were also observed for composites with MCP filling contents of 5%, 10% and 20%.

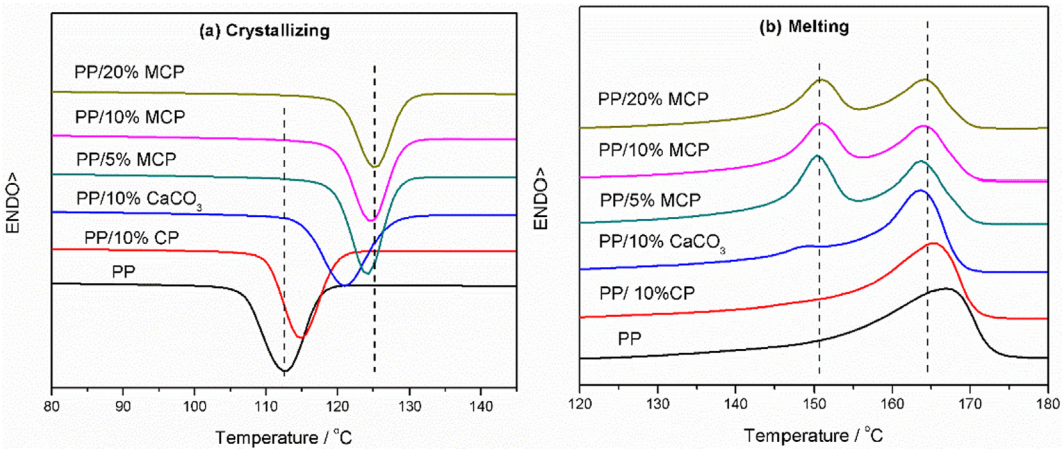

Fig. 6. Crystallizing (a) and melting behavior (b) of PP and the filled composites. (For interpretation of the references to color in this figure legend, the reader is referred to the web version of this article.)

Table 2
Crystallization value for PP and the filled composites.

Samples	T_{onset}/ °C	T_{offset}/ °C	T^{C}_{peak}/ °C	T_m^{β}/ °C	ΔH_{β}/j/g	T_m^{α}/ °C	ΔH_{α}/j/g	K_{β}/%
Neat PP	106.4	119.5	112.33	/	/	167.00	114.5	/
PP/10%CP	109.1	120.9	115.10	/	/	165.00	115.38	/
PP/10% $CaCO_3$	114.1	128.3	121.00	148.33	1.44	163.67	112.34	1.26
PP/10% MCP	118.4	129.7	124.67	151.00	67.41	163.67	50.16	57.33
PP/5% MCP	118.5	129.2	124.33	150.33	73.04	163.67	56.74	56.28
PP/20% MCP	119.2	130.6	125.00	151.00	62.39	164.33	45.91	57.60

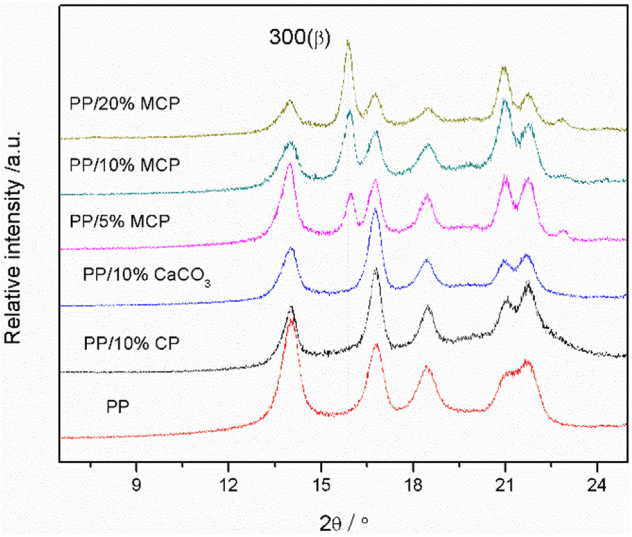

Fig. 7. XRD spectra for PP and the filled composites. (For interpretation of the references to color in this figure legend, the reader is referred to the web version of this article.)

3.6. Nucleating mechanism

The DSC and XRD results demonstrated that the modified cellulose powder was effective in promoting the formation of large fractions of β crystals. The PP β crystal is in a metastable hexagonal form, different from the monoclinic α crystal, posing a "frustrated" structure with different azimuthal settings for the unit cell helices [47]. For β crystal formation, the nucleating agents require specific lattice space to match the PP chains. Thus an epitaxial crystallization process could occur on the surface of the nucleating agent for yielding the oriented β crystals. As illustrated in Fig. 8, the c-cell dimension of isotactic PP chain is 6.5 Å, while the 0 0 1 spacing of pimelate salts is 11.62 Å, which is approximately double of the c-cell distance for PP chain [48,49]. This spacing match provides an ideal lattice arrange for the PP crystallization process. The modified carboxylates are composed of two parts: one is the non-polar hydrocarbon chain, the other is the polar layer connected with celluloses or calcium ions. During the PP crystallization, the melt PP molecular segments are repelled by the polar component and forced into the U ditch of this structure. β nucleus is then formed by PP chains aligned perpendicular to the c-axis of the substrates. Meanwhile, the 7-carbon chains with appropriate spacing constrained the rotation the PP chains and prevented the occurrence of α to β transition. Thus the two parts work together to decrease the free energy and stabilize the formation of β nucleus [49].

3.7. Mechanical property

The mechanical property of the composite is of great importance for the industrial application, and it is meaningful to analyze the effect of crystallization change of the matrix on the mechanical behavior of the cellulose particle filled composites. Table 3 displayed the tensile modulus of pure PP and the filled composites. Neat PP exhibited a low tensile modulus. After filled with 10% particles, the PP/CP, PP/$CaCO_3$, and PP/MCP showed a slight increase of modulus. Generally, thermoplastic materials have a relatively low modulus and the incorporation of hard filler normally increase the modulus of the composite. However, β-PP is reported to have a lower modulus for the small spherulites compared with α-PP [2,50]. In this study, although approximately half of the matrix transformed from α to β crystal PP, the PP/MCP composites still presented a higher modulus than that of neat PP for the incorporation of the rigid MCP particles.

As for the tensile strength of the composites, the stress transfer efficiency at the fiber/matrix interphase is mainly based on the filler dispersion and the interphase bonding. Neat PP showed a tensile strength of 38.51 MPa, similar to the 38.20 MPa from PP/$CaCO_3$, while it decreased to 37.13 MPa after adding the unmodified cellulose particles. The cellulose particles are incompatible with the non-polar matrix and may tend to aggregate in some degree during the melting mixing, leading to poor stress transfer from matrix to particles and decreased the tensile strength. However, the addition of the modified cellulose particles exhibited an increased tensile strength of 40.41 MPa. The surface modification has been shown to decrease the polar nature of the particles and increasing its processability, leading to a more uniform particle dispersion. However, the grafted nucleating sites enhanced the interfacial crystallization by forming small size β spherulites, that may result in an improved particle-matrix adhesion.

The toughness of the PP composites is one of the most import characters when applied in the fields such as automotive industry and furniture market. As showed in Fig. 9, adding 10% $CaCO_3$ or unmodified CP all led to a dramatic decrease of the elongation at break, indicating that the poorly bonded particles could not serve as barriers for the growing cracks and the agglomerates destroyed the continuity of matrix. However, the modified cellulose particles imparted a significant increase of the elongation at break value, from 47% for PP/CP to 403% for PP/MCP, at a 10% filling content. As analyzed above, the modified particles can act as β nucleating agent and induce more than half of the β phase crystal in the matrix, which is known for its excellent toughness. For the PP/MCP composite, the nucleating agent produced a majority of β-PP crystals, making the predominant deformation mechanism change from cavitation to a shear process [51]. This change provided a more fracture-resistance matrix for the composites. Secondly, compared with the α-PP composites, the smaller β crystals presented more tie molecules in the particle/polymer interphase, the β form spherulites are reported to be equipped with a sheaf-like structure, and the lamellae bundles tend to cross each other between the neighboring spherulites, leading to a better interfacial adhesion [52]. Finally, the β phase crystals can undergo a transformation into α phase crystals during deformation and absorb more energy [18,50], resulting in a toughened composite.

The effect of the MCP filling concentrations on the tensile performance was also investigated. The tensile modulus increased as increasing the MCP content, due to the increased fraction of the hard particles. Meanwhile, the tensile strength and elongation at break of the filled samples decreased as raising the particle loadings, especially for 20% particles filled samples, which presented dramatic decreases. For different filler levels, the β phase crystal fraction of the matrix changed

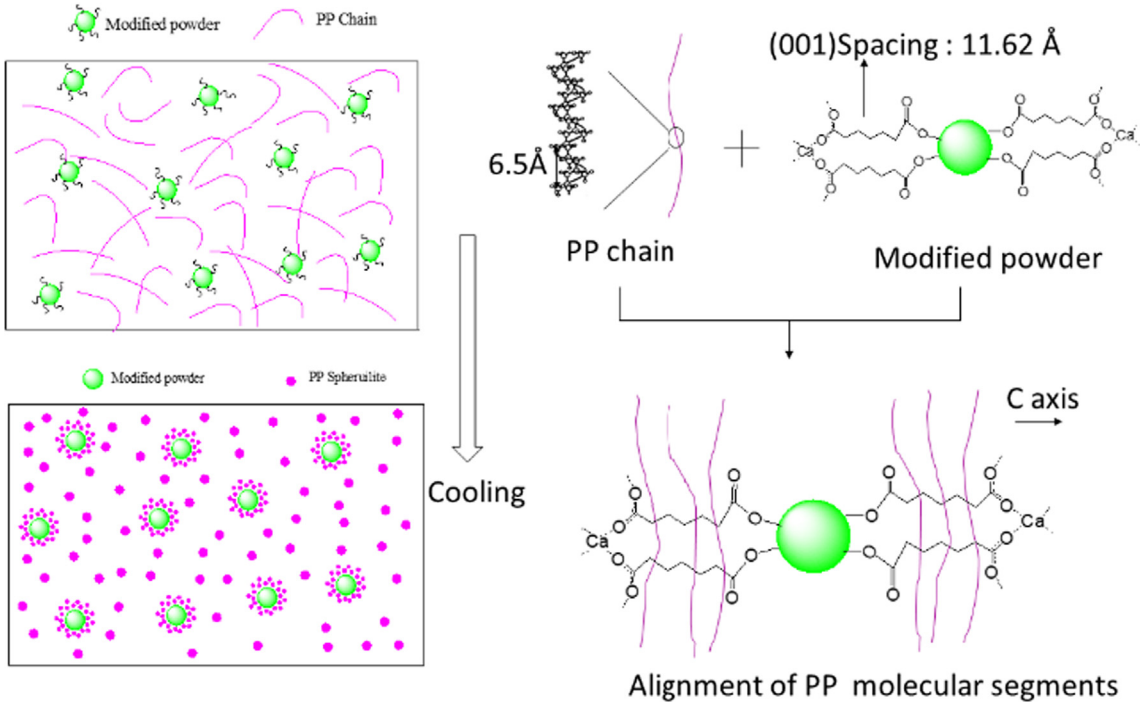

Fig. 8. The proposed arrangement of PP chains around functional groups. (For interpretation of the references to color in this figure legend, the reader is referred to the web version of this article.)

little. Therefore, the β phase crystal content was no longer the limiting factor determining the tensile performance. At a low particle loading, the filler showed excellent stress transfer efficiency, for well-dispersed particles and strong interfacial adhesion. Thus 5% PP/MCP composites showed the highest tensile strength and elongation at break compared with 10% and 20% PP/MCP composites. However, high filler concentrations (20%) may cause filler dispersion problem from the particles aggregation, leading to poor interfacial property and resulted in the decreases of the tensile strength and elongation at break.

3.8. Crystallization morphology

The crystal morphology of the neat PP and the composites were observed under the polarized optical microscopy. From Fig. 10, pure PP spherulites with large diameters were observed. The pure PP crystallization followed a homogeneous nucleation process, where nuclei are difficult to form and the spherulites grow slowly, making the spherulites very large before impinged upon another one. Most of the spherulites showed diameters around 100 μm, as is typical with the α phase. When 10% of cellulose particles were added into the PP matrix, the small powders act as heterogeneous nucleating agents, providing a large number of nucleus for the crystallization, thus the spherulites sizes cannot grow large enough to overlap. Also, because of the presence of the filling particles, the crystal growth was restricted to the particle directions and layer spherulites were formed around the particles. After incorporated with the modified particles, the β phase crystal exhibited a different morphology under polarized light microscopy. The crystal size was decreased significantly and the boundary between spherulites became unclear, demonstrating that the strong β nucleating ability of the modified cellulose particles, which is also in good agreement with the DSC and XRD analysis.

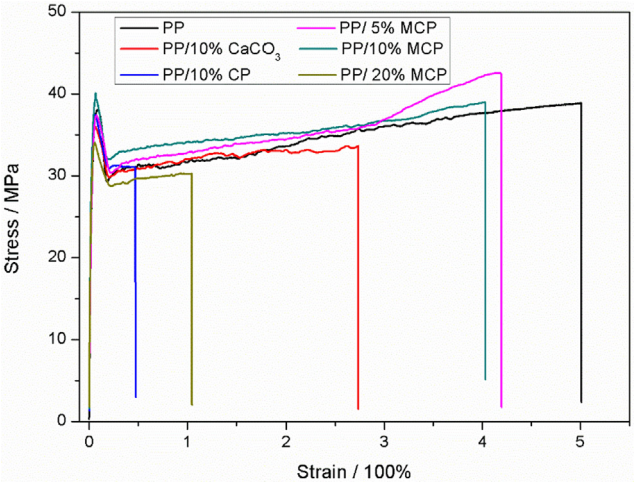

Fig. 9. Stress-strain curves of PP and the filled composites. (For interpretation of the references to color in this figure legend, the reader is referred to the web version of this article.)

4. Conclusions

In this study, the reaction of pimelic acid, calcium carbonate with

Table 3
Tensile properties of the composites.

	PP	PP/10% $CaCO_3$	PP/10% CP	PP/10% MCP	PP/5% MCP	PP/20% MCP
Tensile modulus/GPa	1.54 ± 0.06	1.7 ± 0.10	1.75 ± 0.05	1.72 ± 0.13	1.59 ± 0.04	1.78 ± 0.09
Tensile strength/MPa	38.51 ± 0.32	38.2 ± 0.61	37.13 ± 0.40	40.41 ± 0.69	43.23 ± 0.88	33.42 ± 0.73
Elongation at break/%	501 ± 6	272 ± 26	47 ± 20	403 ± 40	422 ± 28	103 ± 73

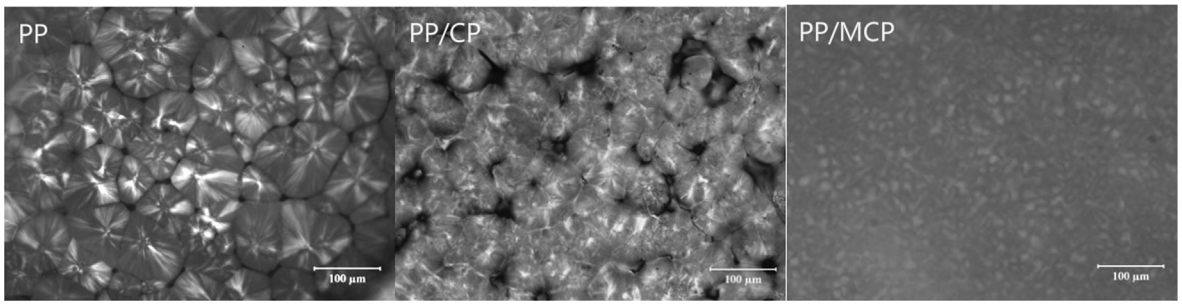

Fig. 10. Polarized light microphotographs of PP and the filled composites.

cellulose for inducing the β nucleating functionalized powders were successfully conducted using a mechnochemical method. The results from FTIR, NMR and TGA revealed that pimelate salts and cellulose esters were formed during the milling reaction. After modification, the dried cellulose powders were compounding with PP to prepare the composites. DSC and XRD analysis showed that the modified particles were effective to produce large percentage (> 50%) of β crystals. Also, the crystallization result showed that the modified samples increased the crystallization temperature and promoted the crystallization rate. The mechanical performance demonstrated the tensile strength and elongation at break of the modified particles filled composites are greatly improved compared with the unmodified ones, due to the small-sized spherulite matrix and the improved interfacial adhesion. As to the filling content, 5% MCP composite exhibited the highest tensile strength and elongation at break, while increasing the filler concentration to 20% led to particle agglomerates and decreased the tensile strength and elongation at break.

The mechanochemical modification of the cellulose particles altered the PP matrix nucleating process, induced the small β-PP spherulite from the dominated α-PP and changed the interfacial connecting structure, therefore leading to a significant improvement of the toughness of the CP/PP composite. This study provides a new route to prepare property-enhanced fiber/PP composite by modifying the interfacial matrix spherulite morphology.

Declaration of Competing Interest

The authors declare that they have no known competing financial interests or personal relationships that could have appeared to influence the work reported in this paper.

Acknowledgment

The authors would like to thank the financial support from the Center for Bioplastics and Biocomposites (CB2), a National Science Foundation Industry, United States/University Cooperative Research Center (Award IIP-#1439732), the Louisiana pacific quasi-Endowment, China Postdoctoral Fund (2019M652504), Postdoctoral innovation project of Shandong province (201902039), and Key Laboratory of Multiphase Flow Reaction and Separation Engineering of Shandong Province (2019MFRS E-B01) for the financial support.

References

[1] Faruk O, Bledzki AK, Fink H-P, Sain M. Biocomposites reinforced with natural fibers: 2000–2010. Prog Polym Sci 2012;37(11):1552–96.
[2] Huang L, Wu Q, Li S, Ou R, Wang Q. Toughness and crystallization enhancement in wood fiber-reinforced polypropylene composite through controlling matrix nucleation. J Mater Sci 2018;53(9):6542–51.
[3] Ganster J, Fink H-P, Pinnow M. High-tenacity man-made cellulose fibre reinforced thermoplastics–injection moulding compounds with polypropylene and alternative matrices. Compos A Appl Sci Manuf 2006;37(10):1796–804.
[4] Ganster J, Fink H-P. Novel cellulose fibre reinforced thermoplastic materials. Cellulose 2006;13(3):271–80.
[5] Ganster J, Fink H-P, Uihlein K, Zimmerer B. Cellulose man-made fibre reinforced polypropylene—correlations between fibre and composite properties. Cellulose 2008;15(4):561–9.
[6] Quillin DT, Caulfield DF, Koutsky JA. Crystallinity in the polypropylene/cellulose system. I. Nucleation and crystalline morphology. J Appl Polym Sci 1993;50(7):1187–94.
[7] Nielsen AS, Pyrz R. A Raman study into the effect of transcrystallisation on thermal stresses in embedded single fibres. J Mater Sci 2003;38(3):597–601.
[8] Varga J, Ehrenstein GW. Beta-modification of isotactic polypropylene. Polypropylene. Springer; 1999. p. 51–9.
[9] Nakamura K, Shimizu S, Umemoto S, Thierry A, Lotz B, Okui N. Temperature dependence of crystal growth rate for [alpha] and [beta] forms of isotactic polypropylene. Polym J (Tokyo, Jpn) 2008;40(9):915.
[10] Foresta T, Piccarolo S, Goldbeck-Wood G. Competition between α and γ phases in isotactic polypropylene: effects of ethylene content and nucleating agents at different cooling rates. Polymer 2001;42(3):1167–76.
[11] Tjong S, Shen J, Li R. Impact fracture toughness of β-form polypropylene. Scr Metall Mater 1995;33(3):503–8.
[12] Tjong S, Li R, Cheung T. Mechanical behavior of CaCO3 particulate-filled β-crystalline phase polypropylene composites. Polym Eng Sci 1997;37(1):166–72.
[13] Dai X, Zhang Z, Wang C, Ding Q, Jiang J, Mai K. A novel montmorillonite with β-nucleating surface for enhancing β-crystallization of isotactic polypropylene. Compos A Appl Sci Manuf 2013;49:1–8.
[14] Zhao S, Cai Z, Xin Z. A highly active novel β-nucleating agent for isotactic polypropylene. Polymer 2008;49(11):2745–54.
[15] Tang J, Wang Y, Liu H, Belfiore LA. Effects of organic nucleating agents and zinc oxide nanoparticles on isotactic polypropylene crystallization. Polymer 2004;45(7):2081–91.
[16] Naffakh M, Marco C, Ellis G. Novel polypropylene/inorganic fullerene-like WS2 nanocomposites containing a β-nucleating agent: isothermal crystallization and melting behavior. J Phys Chem B 2012;116(6):1788–95.
[17] Zhang Z, Chen C, Wang C, Junping Z, Mai K. A novel highly efficient β-nucleating agent for polypropylene using nano-CaCO3 as a support. Polym Int 2010;59(9):1199–204.
[18] Varga J. β-Modification of isotactic polypropylene: preparation, structure, processing, properties, and application. J Macromol Sci, Part B 2002;41(4–6):1121–71.
[19] Garbarczyk J, Paukszta D. Influence of additives on the structure and properties of polymers. Colloid Polym Sci 1985;263(12):985–90.
[20] Varga J, Menyhard A. Effect of solubility and nucleating duality of N, N '-dicyclohexyl-2, 6-naphthalenedicarboxamide on the supermolecular structure of isotactic polypropylene. Macromolecules 2007;40(7):2422–31.
[21] Meng M-R, Dou Q. Effect of pimelic acid on the crystallization, morphology and mechanical properties of polypropylene/wollastonite composites. Mater Sci Eng, A 2008;492(1):177–84.
[22] Gonzalez-Calderon J, Castrejon-Gonzalez E, Medellin-Rodriguez F, Stribeck N, Almendarez-Camarillo A. Functionalization of multi-walled carbon nanotubes (MWCNTs) with pimelic acid molecules: effect of linkage on β-crystal formation in an isotactic polypropylene (iPP) matrix. J Mater Sci 2015;50(3):1457–68.
[23] Wang S-W, Yang W, Bao R-Y, Wang B, Xie B-H, Yang M-B. The enhanced nucleating ability of carbon nanotube-supported β-nucleating agent in isotactic polypropylene. Colloid Polym Sci 2010;288(6):681–8.
[24] Li X, Tabil LG, Panigrahi S. Chemical treatments of natural fiber for use in natural fiber-reinforced composites: a review. J Polym Environ 2007;15(1):25–33.
[25] Sgriccia N, Hawley M, Misra M. Characterization of natural fiber surfaces and natural fiber composites. Compos A Appl Sci Manuf 2008;39(10):1632–7.
[26] Ku H, Wang H, Pattarachaiyakoop N, Trada M. A review on the tensile properties of natural fiber reinforced polymer composites. Compos B Eng 2011;42(4):856–73.
[27] Bahners T, Kelch M, Gebert B, Barajas XLO, Schmidt TC, Gutmann JS, et al. Improvement of fibre–matrix adhesion in cellulose/polyolefin composite materials by means of photo-chemical fibre surface modification. Cellulose 2018;25(4):2451–71.
[28] Hajlane A, Kaddami H, Joffe R. Chemical modification of regenerated cellulose fibres by cellulose nano-crystals: Towards hierarchical structure for structural composites reinforcement. Ind Crops Prod 2017;100:41–50.
[29] Huang L, Mu B, Yi X, Li S, Wang Q. Sustainable use of coffee husks for reinforcing polyethylene composites. J Polym Environ 2018;26(1):48–58.
[30] Klemm D, Philipp B, Heinze T, Heinze U, Wagenknecht W. General considerations on structure and reactivity of cellulose: section 2.1–2.1. 4. Wiley Online Library;

2004.
[31] Kennedy JF, Phillips G, Wedlock D, Williams P. Cellulose and its derivatives: chemistry, biochemistry and applications. Horwood; 1985.
[32] Stone J, Scallan A. A structural model for the cell wall of water-swollen wood pulp fibres based on their accessibility to macromolecules. Cellul Chem Technol 1968;2:343–58.
[33] Fidale LC, Ruiz N, Heinze T, Seoud OAE. Cellulose swelling by aprotic and protic solvents: what are the similarities and differences? Macromol Chem Phys 2008;209(12):1240–54.
[34] Thuresson K, Lindman B, Nyström B. Effect of hydrophobic modification of a nonionic cellulose derivative on the interaction with surfactants. Rheology. J Phys Chem B 1997;101(33):6450–9.
[35] Huang L, Wu Q, Wang Q, Wolcott M. Mechanical activation and characterization of micronized cellulose particles from pulp fiber. Ind Crops Prod 2019;141:111750.
[36] Segal L, Creely J, Martin Jr A, Conrad C. An empirical method for estimating the degree of crystallinity of native cellulose using the X-ray diffractometer. Text Res J 1959;29(10):786–94.
[37] Ou R, Zhao H, Sui S, Song Y, Wang Q. Reinforcing effects of Kevlar fiber on the mechanical properties of wood-flour/high-density-polyethylene composites. Compos A Appl Sci Manuf 2010;41(9):1272–8.
[38] Isogai A, Usuda M, Kato T, Uryu T, Atalla RH. Solid-state CP/MAS carbon-13 NMR study of cellulose polymorphs. Macromolecules 1989;22(7):3168–72.
[39] Morán JI, Alvarez VA, Cyras VP, Vázquez A. Extraction of cellulose and preparation of nanocellulose from sisal fibers. Cellulose 2008;15(1):149–59.
[40] Ibrahim MM, El-Zawawy WK, Nassar MA. Synthesis and characterization of polyvinyl alcohol/nanospherical cellulose particle films. Carbohydr Polym 2010;79(3):694–9.
[41] Kono H, Yunoki S, Shikano T, Fujiwara M, Erata T, Takai M. CP/MAS 13C NMR study of cellulose and cellulose derivatives. 1. Complete assignment of the CP/MAS 13C NMR spectrum of the native cellulose. J Am Chem Soc 2002;124(25):7506–11.
[42] Tingaut P, Zimmermann T, Lopez-Suevos F. Synthesis and characterization of bionanocomposites with tunable properties from poly (lactic acid) and acetylated microfibrillated cellulose. Biomacromolecules 2009;11(2):454–64.
[43] Huang L, Wu Q, Wang Q, Wolcott M. One-step activation and surface fatty acylation of cellulose fibers in a solvent-free condition. ACS Sustainable Chem Eng 2019.
[44] Janicek M, Krejci O, Cermak R. Thermal stability of surface-esterified cellulose and its composite with polyolefinic matrix. Cellulose 2013;20(6):2745–55.
[45] Huang L, Wang H, Wang W, Wang Q, Song Y. Non-isothermal crystallization kinetics of wood-flour/polypropylene composites in the presence of β-nucleating agent. J For Res 2016;27(4):949–58.
[46] Gahleitner M, Grein C, Kheirandish S, Wolfschwenger J. Nucleation of polypropylene homo-and copolymers. Int Polym Process 2011;26(1):2–20.
[47] Stocker W, Schumacher M, Graff S, Thierry A, Wittmann J-C, Lotz B. Epitaxial crystallization and AFM investigation of a frustrated polymer structure: isotactic poly (propylene), β phase. Macromolecules 1998;31(3):807–14.
[48] Yoshimoto S, Ueda T, Yamanaka K, Kawaguchi A, Tobita E, Haruna T. Epitaxial act of sodium 2, 2′-methylene-bis-(4, 6-di-t-butylphenylene) phosphate on isotactic polypropylene. Polymer 2001;42(23):9627–31.
[49] Li X, Hu K, Ji M, Huang Y, Zhou G. Calcium dicarboxylates nucleation of β-polypropylene. J Appl Polym Sci 2002;86(3):633–8.
[50] Tjong S, Shen J, Li R. Morphological behaviour and instrumented dart impact properties of β-crystalline-phase polypropylene. Polymer 1996;37(12):2309–16.
[51] Zhang M, Xu J, Zhang Z, Zeng H, Xiong X. Effect of transcrystallinity on tensile behaviour of discontinuous carbon fibre reinforced semicrystalline thermoplastic composites. Polymer 1996;37(23):5151–8.
[52] Jacoby P. Beta nucleating masterbatch offers enhanced properties in polypropylene products. Plast, Addit Compound 2007;9(3):32–5.